

**You might find this additional information useful...**

---

This article cites 37 articles, 15 of which you can access free at:  
<http://jn.physiology.org/cgi/content/full/78/4/1903#BIBL>

This article has been cited by 8 other HighWire hosted articles, the first 5 are:

**M1 and M2 Muscarinic Acetylcholine Receptor Subtypes Mediate Ca<sup>2+</sup> Channel Current Inhibition in Rat Sympathetic Stellate Ganglion Neurons**

Q. Yang, A. D. Sumner, H. L. Puhl and V. Ruiz-Velasco  
*J Neurophysiol*, November 1, 2006; 96 (5): 2479-2487.  
[\[Abstract\]](#) [\[Full Text\]](#) [\[PDF\]](#)

**{sigma} Receptor Activation Blocks Potassium Channels and Depresses Neuroexcitability in Rat Intracardiac Neurons**

H. Zhang and J. Cuevas  
*J. Pharmacol. Exp. Ther.*, June 1, 2005; 313 (3): 1387-1396.  
[\[Abstract\]](#) [\[Full Text\]](#) [\[PDF\]](#)

**Cholinergic Control of Firing Pattern and Neurotransmission in Rat Neostriatal Projection Neurons: Role of CaV2.1 and CaV2.2 Ca<sup>2+</sup> Channels**

T. Perez-Rosello, A. Figueroa, H. Salgado, C. Vilchis, F. Tecuapetla, J. N. Guzman, E. Galarraga and J. Bargas  
*J Neurophysiol*, May 1, 2005; 93 (5): 2507-2519.  
[\[Abstract\]](#) [\[Full Text\]](#) [\[PDF\]](#)

**Muscarinic and Nicotinic ACh Receptor Activation Differentially Mobilize Ca<sup>2+</sup> in Rat Intracardiac Ganglion Neurons**

F. Beker, M. Weber, R. H. A. Fink and D. J. Adams  
*J Neurophysiol*, September 1, 2003; 90 (3): 1956-1964.  
[\[Abstract\]](#) [\[Full Text\]](#) [\[PDF\]](#)

**Presynaptic Muscarinic M2-Receptor-Mediated Inhibition of N-Type Ca<sup>2+</sup> Channels in Cultured Sphenopalatine Ganglion: Direct Evidence for Acetylcholine Inhibition of Cerebral Nitroergic Neurogenic Vasodilation**

J. Liu, M. S. Evans and T. J.-F. Lee  
*J. Pharmacol. Exp. Ther.*, July 1, 2002; 302 (1): 397-405.  
[\[Abstract\]](#) [\[Full Text\]](#) [\[PDF\]](#)

Medline items on this article's topics can be found at <http://highwire.stanford.edu/lists/artbytopic.dtl> on the following topics:

Physiology .. Calcium Channel  
Oncology .. Muscarinic Receptors  
Neuroscience .. Muscarinic Agonists/Antagonists  
Pharmacology .. Muscarinic Agonists  
Physiology .. Receptor Activation  
Physiology .. Rats

Updated information and services including high-resolution figures, can be found at:  
<http://jn.physiology.org/cgi/content/full/78/4/1903>

Additional material and information about *Journal of Neurophysiology* can be found at:  
<http://www.the-aps.org/publications/jn>

---

This information is current as of November 25, 2009 .

# M<sub>4</sub> Muscarinic Receptor Activation Modulates Calcium Channel Currents in Rat Intracardiac Neurons

J. CUEVAS AND D. J. ADAMS

*Department of Molecular and Cellular Pharmacology, University of Miami School of Medicine, Miami, Florida 33101; and Department of Physiology and Pharmacology, University of Queensland, Brisbane, Queensland 4072, Australia*

**Cuevas, J. and Adams, D. J.** M<sub>4</sub> muscarinic receptor activation modulates calcium channel currents in rat intracardiac neurons. *J. Neurophysiol.* 78: 1903–1912, 1997. Modulation of high-voltage-activated Ca<sup>2+</sup> channels by muscarinic receptor agonists was investigated in isolated parasympathetic neurons of neonatal rat intracardiac ganglia using the amphotericin B perforated-patch whole cell recording configuration of the patch-clamp technique. Focal application of the muscarinic agonists acetylcholine (ACh), muscarine, and oxotremorine-M to the voltage-clamped soma membrane reversibly depressed peak Ca<sup>2+</sup> channel current amplitude. The dose-response relationship obtained for ACh-induced inhibition of Ba<sup>2+</sup> current (*I*<sub>Ba</sub>) exhibited a half-maximal inhibition at 6 nM. Maximal inhibition of *I*<sub>Ba</sub> amplitude obtained with 100 μM ACh was ~75% compared with control at +10 mV. Muscarinic agonist-induced attenuation of Ca<sup>2+</sup> channel currents was inhibited by the muscarinic receptor antagonists pirenzepine (≤300 nM) and m4-toxin (≤100 nM), but not by AF-DX 116 (300 nM) or m1-toxin (60 nM). The dose-response relationship obtained for antagonism of muscarine-induced inhibition of *I*<sub>Ba</sub> by m4-toxin gave an IC<sub>50</sub> of 11 nM. These results suggest that muscarinic agonist-induced inhibition of high-voltage-activated Ca<sup>2+</sup> channels in rat intracardiac neurons is mediated by the M<sub>4</sub> muscarinic receptor. M<sub>4</sub> receptor activation shifted the voltage dependence and depressed maximal activation of Ca<sup>2+</sup> channels but had no effect on the steady-state inactivation of Ca<sup>2+</sup> channels. Peak Ca<sup>2+</sup> channel tail current amplitude was reduced ≥30% at +90 mV in the presence of ACh, indicating a voltage-independent component to the muscarinic receptor-mediated inhibition. Both dihydropyridine- and ω-conotoxin GVIA-sensitive and -insensitive Ca<sup>2+</sup> channels were inhibited by ACh, suggesting that the M<sub>4</sub> muscarinic receptor is coupled to multiple Ca<sup>2+</sup> channel subtypes in these neurons. Inhibition of *I*<sub>Ba</sub> amplitude by muscarinic agonists was also observed after cell dialysis using the conventional whole cell recording configuration. However, internal perfusion of the cell with 100 μM guanosine 5'-O-(2-thiodiphosphate) trilithium salt (GDP-β-S) or incubation of the neurons in Pertussis toxin (PTX) abolished the modulation of *I*<sub>Ba</sub> by muscarinic receptor agonists, suggesting the involvement of a PTX-sensitive G-protein in the signal transduction pathway. Given that ACh is the principal neurotransmitter mediating vagal innervation of the heart, the presence of this inhibitory mechanism in postganglionic intracardiac neurons suggests that it may serve for negative feedback regulation.

## INTRODUCTION

Four muscarinic receptor genes (m1–m4) have been detected in guinea pig and rat intrinsic cardiac neurons using *in situ* hybridization (Hassall et al. 1993; Hoover et al. 1994). These genes correspond to the pharmacologically defined M<sub>1</sub>–M<sub>4</sub> muscarinic receptor subtypes (Hulme et al. 1990). To date, three different muscarinic ACh receptor

(mAChR)-induced voltage responses have been observed in guinea pig intracardiac neurons: two temporally distinct depolarizations and a slow hyperpolarization (Allen and Burnstock 1990; Mihara et al. 1988). The faster depolarization is believed to be associated with a decrease in K<sup>+</sup> permeability, whereas the slower depolarization and the hyperpolarization with increases in a Cl<sup>-</sup> and a K<sup>+</sup> conductance, respectively (Allen et al. 1994). Acetylcholine (ACh) activation of muscarinic receptors also decreases the amplitude of the tetrodotoxin (TTX)-insensitive component of the action potential and Ca<sup>2+</sup>-dependent afterhyperpolarization in guinea pig cultured intracardiac neurons (Allen and Burnstock 1990), consistent with a decrease in Ca<sup>2+</sup> influx through voltage-dependent Ca<sup>2+</sup> channels. Inhibition of depolarization-activated Ca<sup>2+</sup> channel currents by muscarine has been observed in mammalian central and peripheral neurons, including sympathetic neurons of rat superior cervical ganglia (Mathie et al. 1992; Wanke et al. 1987) and rat hippocampal pyramidal neurons (Gähwiler and Brown 1987). Muscarinic receptor-mediated Ca<sup>2+</sup> channel inhibition has also been observed in amphibian parasympathetic neurons of the interatrial septum of the bullfrog heart (Tse et al. 1990). However, muscarinic receptor modulation of voltage-dependent Ca<sup>2+</sup> channels has not been investigated in parasympathetic neurons of mammalian intracardiac ganglia.

Both muscarinic and α-adrenergic receptor activation have been shown to suppress vagal-induced ACh release from rat cardiac parasympathetic nerve fibers (McDonough et al. 1986; Manabe et al. 1991; Wetzel et al. 1985). The mechanism proposed to underlie α-adrenergic inhibition of ACh release is α-adrenoreceptor-induced attenuation of N-type Ca<sup>2+</sup> channels, which has been described in isolated rat intracardiac neurons (Xu and Adams 1993). However, the mechanism involved in muscarinic receptor-mediated inhibition of vagal-induced ACh release in rat parasympathetic cardiac neurons has not been investigated. Furthermore, in contrast to α-adrenoreceptor activation, which inhibits primarily N-type Ca<sup>2+</sup> channels, muscarinic receptor activation has been shown to also modulate L-type Ca<sup>2+</sup> channels in rat sympathetic neurons (Mathie et al. 1992).

Both M<sub>1</sub> and M<sub>4</sub> muscarinic receptors appear to mediate ACh inhibition of Ca<sup>2+</sup> channels in rat sympathetic neurons (Bernheim et al. 1992). Precise identification of muscarinic receptor subtypes has been hampered by the lack of specific receptor antagonists. Recently, toxins highly selective for M<sub>1</sub> and M<sub>4</sub> muscarinic receptors have been isolated from

the venom of the green mamba (Jolkkonen et al. 1994; Max et al. 1993a,b), facilitating the separation of membrane responses evoked by activation of different muscarinic receptor subtypes. The coupling of these receptors to  $\text{Ca}^{2+}$  channels has been shown to involve different signal transduction pathways in rat sympathetic neurons, which include both pertussis toxin-sensitive and -insensitive G-proteins (Beech et al. 1991; Bernheim et al. 1991, 1992). In the present study, muscarinic ACh receptor modulation of depolarization-activated  $\text{Ca}^{2+}$  channels was investigated in isolated parasympathetic neurons from rat intracardiac ganglia. ACh reversibly inhibited  $\text{Ca}^{2+}$  channel currents via activation of an  $M_4$  muscarinic receptor, which is coupled to a pertussis toxin-sensitive G-protein and modulates multiple  $\text{Ca}^{2+}$  channel types in these neurons. A preliminary report of some of these results has been presented as an abstract (Cuevas and Adams 1995).

## METHODS

### Preparation

Isolated parasympathetic neurons, dissociated from neonatal rat intracardiac ganglia, were obtained and cultured as described previously (Fieber and Adams 1991). Briefly, atria were dissected from neonatal rats (3–8 days old), killed by decapitation, and incubated in a Krebs solution containing 1 mg/ml collagenase (Type 2; Worthington Biomedical, Freehold, NJ) for 1 h at 37°C. Individual ganglia were dissected from the epicardial ganglion plexus, transferred to a culture dish containing a high glucose medium (Dulbecco's Modified Eagle Media, 10% fetal calf serum, 100 U/ml penicillin, and 0.1 mg/ml streptomycin), titrated with a fine bore pasteur pipette and plated onto 18-mm glass coverslips coated with laminin. The dissociated cells were incubated at 37°C in 95%  $\text{O}_2$ -5%  $\text{CO}_2$  atmosphere and used for experiments within 24–72 h. At the time of experiments, the glass coverslip was

transferred to a recording chamber (0.5 ml volume) and viewed at  $\times 400$  magnification using an inverted phase contrast microscope.

### Current recording

Membrane currents were recorded from voltage-clamped neurons using the whole cell recording configuration of the patch-clamp technique (Hamill et al. 1981). Patch pipettes (1–3 M $\Omega$ ) were pulled from thin-walled borosilicate glass (GC150TF; Clark Electromedical Instruments, Reading, UK) and fire polished. Electrical access was achieved either by rupturing the membrane patch and dialyzing the cell, or through the perforated-patch method using amphotericin B (Rae et al. 1991). The perforated-patch method was used to preserve the intracellular integrity of the neurons, thus maintaining functional muscarinic ACh responses lost after cell dialysis in these neurons. For perforated-patch experiments, a stock solution of amphotericin B (60 mg/ml) in dimethylsulfoxide (DMSO) was prepared and diluted in the pipette solution immediately before use yielding a final concentration of 360  $\mu\text{g/ml}$  amphotericin B in 0.6% DMSO. Antibiotic incorporation into the membrane patch was monitored by applying a  $-10$ -mV pulse at 1 Hz from a holding potential of  $-70$  mV, and, in successful experiments, the appearance of a slow capacitive transient and a decrease in the series resistance ( $R_s$ ) to  $< 10$  M $\Omega$  was observed. To minimize voltage error,  $R_s$  was typically compensated by 50% to  $\leq 5$  M $\Omega$ .

Depolarization-activated  $\text{Ca}^{2+}$  channel currents were elicited using voltage steps from  $-90$  mV to more positive potentials applied every 10–20 s. Capacitive and leak currents were subtracted using the  $-P/4$  pulse protocol, which assumes a linear relationship for these currents at voltages less than  $-90$  mV (Xu and Adams 1992). Membrane currents were amplified using an Axopatch 200A patch-clamp amplifier (Axon Instruments, Foster City, CA), filtered at 10 kHz ( $-3$  dB) with a 4-pole Bessel filter, and digitized at 50 kHz (Digidata 1200A, Axon Instruments). A PC Pentium/75 MHz computer running pClamp programs (Axon Instruments) was used to generate voltage pulses and to acquire and analyze data.

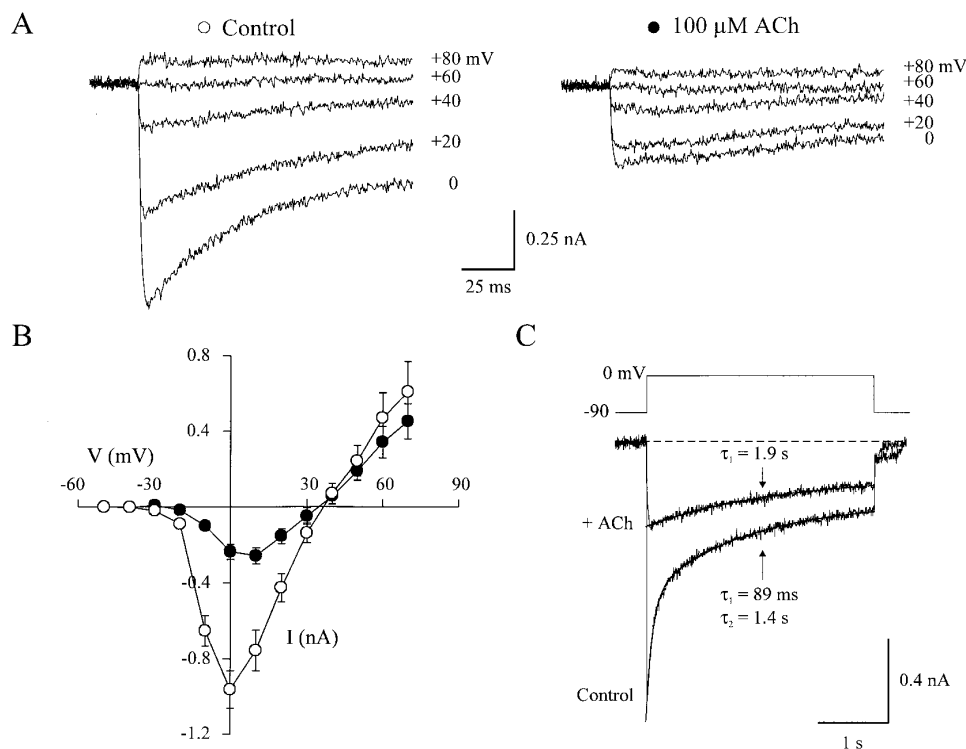


FIG. 1. Acetylcholine (ACh)-mediated inhibition of high-voltage-activated  $\text{Ca}^{2+}$  channel currents in rat parasympathetic neurons. **A**: family of  $\text{Ba}^{2+}$  currents evoked in the absence ( $\circ$ ) and presence ( $\bullet$ ) of 100  $\mu\text{M}$  ACh. Holding potential,  $-90$  mV. **B**: whole cell current-voltage ( $I$ - $V$ ) relation of peak  $\text{Ba}^{2+}$  current amplitude obtained in the absence ( $\circ$ ) and presence ( $\bullet$ ) of 100  $\mu\text{M}$  ACh. Data points represent mean  $\pm$  SE for 5 cells. **C**: ACh-mediated effects on the amplitude and time course of decay of  $\text{Ca}^{2+}$  channel currents. Superimposed traces of  $I_{\text{Ba}}$  elicited by depolarizing steps (3 s duration) to 0 mV from  $-90$  mV in the absence (Control) and presence (+ACh) of 100  $\mu\text{M}$  ACh. Solid lines represent best fit of the time course of current decay using either single (+ACh) or the sum of 2 (Control) exponential functions. Mecamylamine (3  $\mu\text{M}$ ) was coapplied with ACh to block nicotinic ACh receptor activation.

Experiments on dialyzed neurons were performed within 20 min of rupturing the membrane patch to minimize the effects of Ca<sup>2+</sup> channel current "run-down," which has been reported using conventional whole cell recording configuration (Xu and Adams 1992). During this time, Ca<sup>2+</sup> channel current amplitude decreased by <10%. Calcium current run-down was not observed in neurons electrically accessed using the perforated-patch recording configuration.

The time course of inactivation of Ca<sup>2+</sup> channel currents were fit using the pClamp program, Clampfit (Axon Instruments), and Boltzmann distributions for determining the voltage dependence of activation and inactivation were fit using SigmaPlot 3.0 (Jandel Scientific, San Rafael, CA). Both programs determined the best fit to the data using the minimum  $\chi^2$  method. Dose-response curves were obtained by measuring peak current amplitudes at each agonist/antagonist concentration, and the experimental data points were fit with the equation

$$I/I_{\max} = 1/[1 + ([A]/IC_{50})^k] + I_0 \quad (1)$$

where  $I/I_{\max}$  is the relative current,  $I_0$  represents the nonreducible current,  $[A]$  is the agonist/antagonist concentration,  $IC_{50}$  is the half-maximal concentration, and  $k$  is the slope parameter. Data points represent mean  $\pm$  SE. Statistical difference was determined using paired  $t$ -test for within group experiments, and unpaired  $t$ -test for between group experiments, and was considered significant if  $P < 0.05$ .

### Solutions and materials

The bath solution (physiological salt solution, PSS) used in these experiments contained (in mM) 140 NaCl, 2.5 CaCl<sub>2</sub>, 1.2 MgCl<sub>2</sub>, 7.7 D-glucose, and 10 4-(2-hydroxyethyl)-1-piperazine ethansulfonic acid (HEPES), adjusted to pH 7.4 with NaOH. Ca<sup>2+</sup> channel currents were obtained in the presence of 300 nM TTX, and Ba<sup>2+</sup> (5 mM) was used as the charge carrier to maximize Ca<sup>2+</sup> channel current amplitude, and to minimize any Ca<sup>2+</sup>-dependent current rundown (Xu and Adams 1992). The pipette solution used for perforated-patch experiments contained (in mM) 75 Cs<sub>2</sub>SO<sub>4</sub>, 55 CsCl, 5 MgSO<sub>4</sub>, and 10 HEPES, pH adjusted to 7.2 with *N*-methyl-D-glucamine; whereas that used for conventional (dialyzed) whole cell recordings contained (in mM) 140 CsCl, 2 MgCl<sub>2</sub>, 2 1,2-bis(2-aminophenoxy)ethane-*N,N,N',N'*-tetraacetic acid (BAPTA) cesium salt, 2 Mg<sub>2</sub> ATP, 0.1 guanosine 5'-triphosphate (GTP) sodium salt, and 10 HEPES, pH adjusted to 7.2 with Cs-OH. The osmolality of the solutions (280–290 mmol/kg) was monitored with a vapor pressure osmometer (Wescor 5500, Logan, UT). Muscarinic ACh-evoked responses were elicited by pressure ejection of either ACh, muscarine, or oxotremorine-M at the concentrations indicated from an extracellular pipette position  $\sim$ 50  $\mu$ m from the cell soma. Mecamylamine (3  $\mu$ M) was coapplied with ACh to inhibit nicotinic ACh receptor activation (Fieber and Adams 1991). The recording chamber was continually perfused ( $\sim$ 2 ml/min) with the indicated bath solutions at 22–23°C. In a series of experiments, external Na<sup>+</sup> (70 mM) was replaced isosmotically by tetraethylammonium ions (TEA) to block outward K<sup>+</sup> channel currents and optimize the recording of Ca<sup>2+</sup> channel tail currents. External TEA, however, shifts the ACh dose-response curve to the right by  $\sim$ 36-fold, without reducing the maximum response attainable (Caulfield 1991). Therefore a maximally effective concentration of 100  $\mu$ M ACh was used in these whole cell experiments. Pharmacological characterization of the muscarinic receptor subtype was carried out using specific muscarinic receptor antagonists: pirenzepine, AF-DX 116, and the green mamba (*Dendroaspis angusticeps*) toxins, m1-toxin and m4-toxin. Muscarinic receptor antagonists were bath applied and/or pressure ejected together with the agonists.

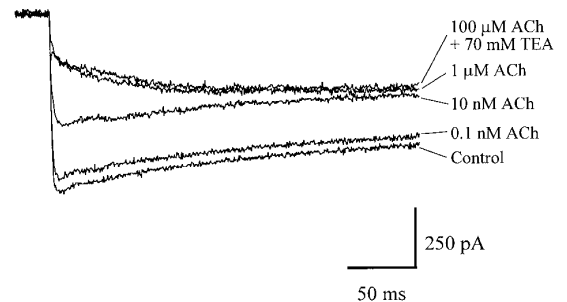
In one series of experiments, 100  $\mu$ M guanosine 5'-O-(2-thiophosphate) trilithium salt (GDP- $\beta$ -S) was substituted for GTP in the pipette solution, and in another series, neurons were preincubated in 200 ng/ml of pertussis toxin (*Bordetella pertussis*; PTX) for 24 h immediately before the experiments.

All chemical reagents used were of analytic grade. The following drugs were used: GDP- $\beta$ -S and GTP obtained from Boehringer Mannheim (Indianapolis, IN); AChCl, amphotericin B, ( $\pm$ )muscarine chloride, and mecamylamine hydrochloride from Sigma Chemical (St Louis, MO); nimodipine, oxotremorine methiodide (oxotremorine-M), and pirenzepine dihydrochloride from Research Biochemicals International (Natick, MA);  $\omega$ -conotoxin GVIA ( $\omega$ -CgTX, *Conus geographus*), TTX, and PTX from Calbiochem (San Diego, CA); and MT-3 (*Dendroaspis angusticeps*) from Alomone Labs. (Jerusalem, Israel). AF-DX 116, m1-toxin, and m4 toxin were a generous gift from Dr. L. T. Potter (University of Miami School of Medicine, Miami, FL). m4-toxin is identical to the recently described muscarinic toxin 3 (MT-3) in amino acid sequence and selectivity for muscarinic m4 receptors (Jolkonen et al. 1994).

### RESULTS

Muscarinic ACh receptor activation modified the active membrane electrical properties of all rat intracardiac neurons

A



B

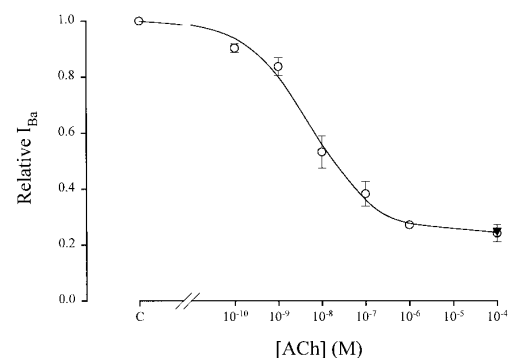


FIG. 2. Dose dependence of ACh-mediated inhibition of high-voltage-activated Ca<sup>2+</sup> channel currents. A: Ba<sup>2+</sup> currents evoked in response to +100-mV depolarization from a holding potential of -90 mV in the absence (Control) and presence ACh and ACh + tetraethylammonium (TEA). Currents were evoked by voltage steps from -90 to +10 mV. Mecamylamine (3  $\mu$ M) was coapplied with ACh. B: relative peak whole cell  $I_{Ba}$  amplitude obtained at +10 mV in the absence ( $\circ$ ) and presence ( $\blacktriangledown$ ) of 70 mM TEA, plotted as a function of ACh concentration. Current amplitude was measured isochronally at the time of the peak of control  $I_{Ba}$  (10 ms after the onset of the voltage step). Data points represent the mean  $\pm$  SE for 6 cells. The curve represents a best fit of the data obtained in the absence of TEA by Eq. 1 with an  $IC_{50} = 5.6$  nM ACh and slope,  $k = 0.6$ .

studied ( $n > 100$ ). Muscarinic receptor activation depolarizes neurons and increases the number of action potentials elicited by depolarizing current pulses without significantly altering action-potential duration (Cuevas et al. 1997). The actions of ACh on resting membrane potential and discharge characteristics have been shown to be mediated by  $M_1$  muscarinic receptor activation. In the present study, we examine the effects of ACh on high-voltage-activated  $Ca^{2+}$  channels.

#### Muscarinic ACh-mediated attenuation of $Ca^{2+}$ channel currents

$Ca^{2+}$  channel currents were isolated by inhibiting depolarization-activated  $Na^+$  currents with extracellular TTX (300 nM), and  $K^+$  channels with intracellular  $Cs^+$  and extracellular TEA and  $Ba^{2+}$  (5 mM).  $Ba^{2+}$  was used as the charge carrier through open  $Ca^{2+}$  channels in most experiments for reasons discussed in METHODS. The effect of ACh on the  $Ba^{2+}$  current-voltage ( $I$ - $V$ ) relationship was examined using brief (100 ms) step depolarizations of 10-mV increments ( $-50$  to  $+90$  mV) from a holding potential of  $-90$  mV. Figure 1A shows a family of high-voltage-activated  $Ba^{2+}$  currents ( $I_{Ba}$ ) obtained in the absence (Control) and presence of  $100 \mu M$  ACh. Focal application of ACh reversibly depressed the peak amplitude and slowed the activation of  $I_{Ba}$  at all test potentials. Figure 1B shows the average  $I$ - $V$  relationship obtained for five neurons. Under control conditions,  $I_{Ba}$  was activated at approximately  $-30$  mV and  $I$ - $V$  relation was maximal at  $0$  mV, reversing at approximately  $+40$  mV. In the presence of ACh, the  $I$ - $V$  relationship exhibited a similar voltage dependence, but the peak  $I_{Ba}$  amplitude was reduced at all voltages. At  $0$  mV,  $I_{Ba}$  was decreased by 75%, from  $-963.3 \pm 99.5$  pA to  $-236.5 \pm 39.6$  pA ( $n = 5$ ), in the absence and presence of ACh, respectively. ACh

inhibition of  $Ca^{2+}$  channel current occurred to a similar degree when  $Ca^{2+}$  was the charge carrier (data not shown).

Figure 1C shows representative  $Ca^{2+}$  channel currents evoked by a 3 s step depolarization to  $0$  mV from a holding potential of  $-90$  mV in the absence and presence of  $100 \mu M$  ACh +  $3 \mu M$  mecamylamine. Under control conditions, the time-dependent inactivation of  $I_{Ba}$  was biphasic, and best fit by the sum of two exponential functions with time constants of  $90$  ms ( $\tau_f$ ) and  $1.40$  s ( $\tau_s$ ). In the presence of ACh, the inward current decay was best fit by a single exponential function with a time constant of  $1.90$  s ( $\tau_s$ ). Bath application of  $100 \mu M$   $Cd^{2+}$  completely blocked the depolarization-activated  $Ba^{2+}$  current both in the absence and the presence of ACh (data not shown). In four similar experiments, the time course of  $I_{Ba}$  decay was best fit by the sum of two exponential functions with mean time constants of  $99 \pm 9$  ms ( $\tau_f$ ) and  $1.35 \pm 0.09$  s ( $\tau_s$ ). In all neurons studied, the decay of  $I_{Ba}$  obtained in the presence of  $100 \mu M$  ACh was best fit by a single exponential function with  $\tau_s = 1.60 \pm 0.21$  s ( $n = 4$ ). The effect of ACh on the time course of decay of  $I_{Ba}$  was reversible on wash out (data not shown).

#### ACh concentration-dependent inhibition of $I_{Ba}$

Focal application of the muscarinic receptor agonists, ACh, muscarine, and oxotremorine-M to the voltage-clamped soma membrane reversibly inhibited whole cell  $I_{Ba}$  amplitude. The dose-response relationship for ACh-induced inhibition of  $Ca^{2+}$  channel currents was examined both in the absence and presence of external TEA. Figure 2A shows superimposed  $Ba^{2+}$  currents evoked by depolarizing pulses to  $+10$  mV from  $-90$  mV obtained in the absence (control) and presence of different ACh concentrations ( $0.1$  nM to  $1 \mu M$ ) and  $100 \mu M$  ACh plus  $70$  mM TEA. Relative peak  $I_{Ba}$  amplitude plotted as a function of ACh concentration is

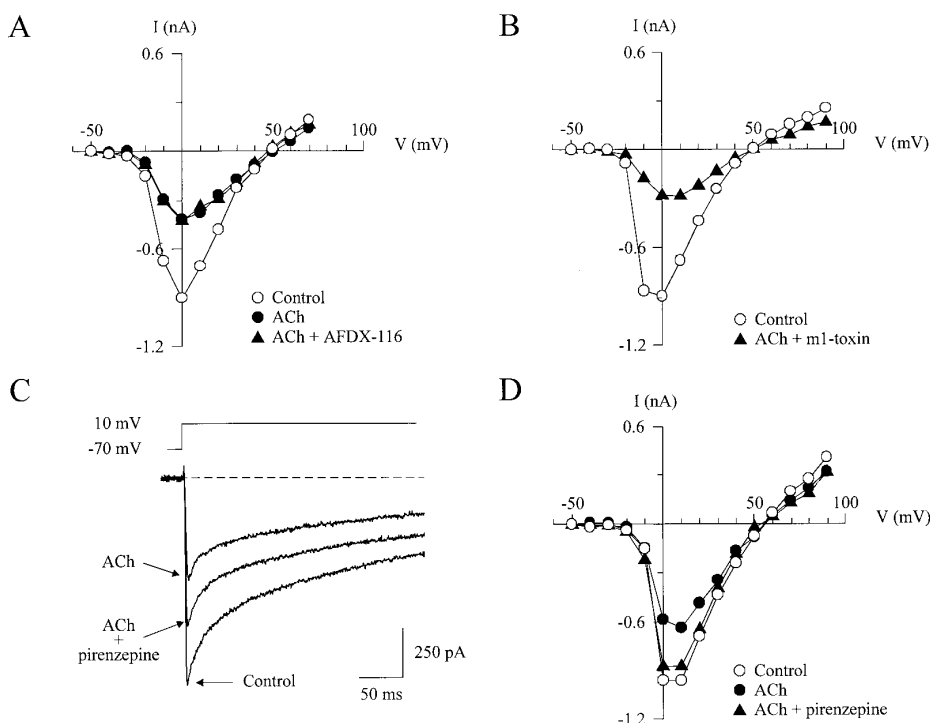


FIG. 3. ACh-mediated inhibition of  $Ca^{2+}$  channel currents is antagonized by  $M_4$ , but not by  $M_1$  or  $M_2$  muscarinic receptor antagonists. *A*: whole cell  $I$ - $V$  relations of peak  $Ba^{2+}$  currents obtained in the absence ( $\circ$ ) of ACh, the presence of  $100 \mu M$  ACh alone ( $\bullet$ ), and in the presence of  $100 \mu M$  ACh +  $300$  nM AF-DX 116 ( $\blacktriangle$ ). *B*:  $I$ - $V$  relations obtained from the same neuron before ( $\circ$ ) and after 10 min incubation in  $1$  U/ml of m1-toxin ( $\blacktriangle$ ). *C*: superimposed whole cell  $I_{Ba}$  elicited by depolarization to  $+10$  mV from  $-70$  mV in the absence (Control) or presence of  $100 \mu M$  ACh, and in the presence of  $100 \mu M$  ACh together with  $100$  nM pirenzepine. *D*: whole cell  $I$ - $V$  relations of peak  $I_{Ba}$  obtained in the absence of ACh ( $\circ$ ), presence of  $100 \mu M$  ACh alone ( $\bullet$ ), and in the presence of  $100 \mu M$  ACh +  $300$  nM pirenzepine ( $\blacktriangle$ ).

shown in Fig. 2B. The dose-reponse relationship obtained for inhibition of  $I_{\text{Ba}}$  by ACh was best fit by Eq. 1 with a half-maximal inhibitory ACh concentration of 6 nM. Maximal inhibition of  $I_{\text{Ba}}$  amplitude was obtained with 100  $\mu\text{M}$  ACh in the absence and presence of 70 mM TEA. Muscarine (5  $\mu\text{M}$ ) and oxotremorine-M (5  $\mu\text{M}$ ) reversibly depressed peak  $I_{\text{Ba}}$  amplitude at 0 mV by  $55 \pm 4\%$  and  $60 \pm 3\%$  ( $n = 3$ ), respectively, compared with control in the presence of external TEA (data not shown).

#### Inhibition of ACh modulation of $I_{\text{Ba}}$ by muscarinic receptor antagonists

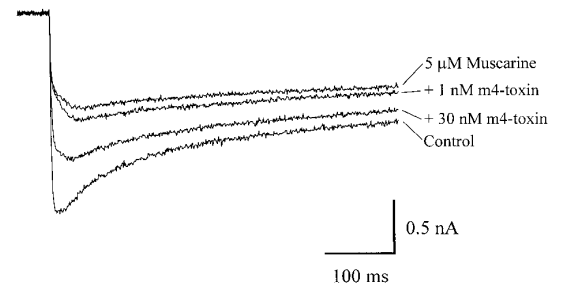
Figure 3A shows peak  $I$ - $V$  relationships for whole cell  $I_{\text{Ba}}$  obtained in the absence and presence of focally applied 100  $\mu\text{M}$  ACh + 3  $\mu\text{M}$  mecamylamine. The ACh-induced decrease in  $I_{\text{Ba}}$  was not affected by bath application of 100 nM AF-DX 116, a selective  $M_2$  muscarinic receptor antagonist (Hulme et al. 1990). AF-DX 116 (300 nM) alone had no effect on either  $I_{\text{Ba}}$  amplitude or time course (data not shown). Figure 3B shows the  $I$ - $V$  relationships obtained in the absence (Control) and presence of bath-applied m1-toxin (60 nM), an irreversible antagonist of the  $M_1$  muscarinic receptor (Max et al. 1993a). Focally applied ACh reduced peak  $I_{\text{Ba}}$  amplitude at all voltages tested in the presence of m1-toxin. ACh-mediated inhibition of peak  $I_{\text{Ba}}$  was, however, partially antagonized by bath application of pirenzepine. Figure 3C shows superimposed inward  $\text{Ba}^{2+}$  currents evoked in response to step depolarizations from  $-90$  to 0 mV in the absence and presence of 100  $\mu\text{M}$  ACh and ACh plus 100 nM pirenzepine. In three similar experiments, ACh-induced inhibition of  $I_{\text{Ba}}$  was reduced by 46% in the presence of 100 nM pirenzepine, decreasing from  $65 \pm 7\%$  (1  $\mu\text{M}$  ACh) to  $35 \pm 3\%$  (1  $\mu\text{M}$  ACh + 100 nM pirenzepine). In the presence of 300 nM pirenzepine, ACh-induced inhibition of  $I_{\text{Ba}}$  was depressed by 81% ( $n = 3$ ), and this antagonism was observed at all voltages tested (Fig. 3D).

The antagonism of muscarine-induced inhibition of  $I_{\text{Ba}}$  was examined using m4-toxin, a specific competitive antagonist of the  $M_4$  muscarinic ACh receptor (Jolkkonen et al. 1994; Max et al. 1993b). Figure 4A shows superimposed  $\text{Ba}^{2+}$  currents evoked in response to a step depolarization to +10 mV from  $-90$  mV obtained in the absence (control) and presence of muscarine and m4-toxin.  $I_{\text{Ba}}$  amplitude was reduced by  $\sim 50\%$  in the presence of 5  $\mu\text{M}$  muscarine, and this inhibition was antagonized by m4-toxin. The dose-response relationship for m4-toxin antagonism of muscarine-induced inhibition of  $I_{\text{Ba}}$  is shown in Fig. 4B. Antagonism of muscarine-induced  $I_{\text{Ba}}$  inhibition by m4-toxin was half-maximal at 11 nM and maximally effective with 1  $\mu\text{M}$  m4-toxin. In four similar experiments, oxotremorine-M inhibition of  $I_{\text{Ba}}$  was completely and reversibly abolished by bath application of 60 nM m4-toxin.

#### Block of ACh-mediated inhibition of $I_{\text{Ba}}$ by GDP- $\beta$ -S and PTX

ACh-mediated inhibition of  $I_{\text{Ba}}$  observed in neurons dialyzed with an intracellular pipette solution containing both 2 mM BAPTA and 0.1 mM GTP was similar to that observed in neurons electrically accessed using the perforated-patch

A



B

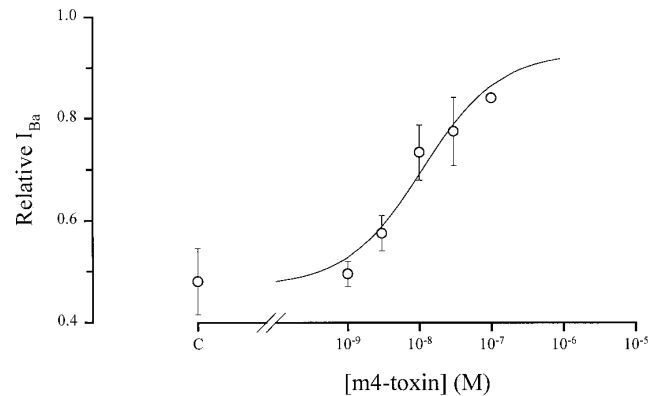


FIG. 4. Dose-dependent antagonism of muscarine-induced inhibition of depolarization-activated  $\text{Ca}^{2+}$  channel currents by m4-toxin. A: superimposed  $\text{Ba}^{2+}$  currents obtained in the absence (Control) and presence 5  $\mu\text{M}$  muscarine and muscarine coapplied with m4-toxin. Currents were evoked by step depolarization to +10 mV from a holding potential of  $-90$  mV. B: dose-response relationship for the displacement of muscarine-induced inhibition by varying concentrations of m4-toxin. Relative peak whole cell  $I_{\text{Ba}}$  amplitude plotted as a function of m4-toxin concentration. Data points represent the mean  $\pm$  SE for 6 cells. The curve represents a best fit of the data by Eq. 1 with half-maximal concentration ( $\text{IC}_{50}$ ) = 11 nM m4-toxin and  $k = -0.8$ .

method. Figure 5A shows representative currents in response to a step depolarization from  $-70$  to 0 mV recorded from a dialyzed neuron in the absence and presence of 100  $\mu\text{M}$  ACh. In dialyzed whole cell recordings, maximal inhibition of  $I_{\text{Ba}}$  by ACh occurred at +10 mV.  $I_{\text{Ba}}$  amplitude decreased by  $\sim 72\%$  in the presence of ACh, from  $-840 \pm 32$  pA (control) to  $-237 \pm 13$  pA (ACh;  $n = 4$ ). Figure 5B shows depolarization-activated  $I_{\text{Ba}}$  recorded from a neuron dialyzed with a pipette solution containing 0.1 mM GDP- $\beta$ -S. Peak  $I_{\text{Ba}}$  amplitude was similar to that recorded from neurons dialyzed with the control pipette solution; however, bath or focal application of ACh had no effect on peak  $I_{\text{Ba}}$  amplitude or activation kinetics. Mean  $I_{\text{Ba}}$  amplitudes, obtained in the absence and presence of 100  $\mu\text{M}$  ACh, were  $-980 \pm 52$  and  $-879 \pm 32$  pA ( $n = 3$ ), respectively. In the presence of GDP- $\beta$ -S, the rate of decay of  $I_{\text{Ba}}$  was decreased in some neurons (Fig. 5B), but ACh failed to inhibit  $I_{\text{Ba}}$  in the presence of GDP- $\beta$ -S in all neurons examined.

$\text{Ba}^{2+}$  currents elicited by voltage steps from  $-70$  to +10 mV in a neuron preincubated in PTX (200 ng/ml, 24 h) are shown in Fig. 5C. ACh failed to inhibit  $I_{\text{Ba}}$  in PTX-treated

neurons, whereby  $I_{Ba}$  amplitude was  $-1.12 \pm 0.11$  nA and  $-1.04 \pm 0.09$  nA ( $n = 3$ ), in the absence and presence of ACh, respectively. A summary of the peak  $I_{Ba}$  amplitudes elicited on depolarization to +10 mV, normalized to their respective control values, under the different experimental

conditions is presented in Fig. 5D. ACh decreased  $I_{Ba}$  by  $72 \pm 1\%$  ( $n = 4$ ) in neurons dialyzed with control pipette solution, which was statistically significant ( $P < 0.03$ ). The peak  $I_{Ba}$  amplitude obtained in the presence of ACh in dialyzed neurons was not statistically different to  $I_{Ba}$  amplitude obtained using the perforated-patch whole cell recording configuration. In neurons dialyzed with GDP- $\beta$ -S,  $I_{Ba}$  was decreased by  $10 \pm 2\%$  ( $n = 4$ ), whereas in neurons preincubated in PTX,  $I_{Ba}$  was reduced by only  $7 \pm 5\%$  ( $n = 3$ ). Neither of these ACh-evoked decreases in  $I_{Ba}$  were statistically significant.

#### Effects of ACh on the voltage dependence of steady-state inactivation and activation

The effect of ACh on steady-state inactivation of  $Ca^{2+}$  channels in rat intracardiac neurons was studied using a double pulse protocol. Neurons were initially held at  $-90$  mV, and 4-s prepulses from  $-120$  to  $+10$  mV were applied in 10-mV increments before a voltage step to  $+20$  mV to activate (open) the available  $Ca^{2+}$  channels. The steady-state inactivation of  $I_{Ba}$  exhibited a sigmoidal dependence on voltage and was best fit with a single Boltzmann function according to the equation

$$I_{Ba} = I_{Ba(max)} / \{1 + \exp[(V - V_h)/k]\}$$

A fit of the mean relative current [ $I_{Ba}/I_{Ba(max)}$ ]-voltage relationship for three neurons exhibited half-maximal steady-state inactivation ( $V_h$ ) at  $-57$  mV under control conditions and  $-54$  mV in the presence of ACh ( $n = 3$ ). The slope parameter ( $k$ ) was  $-13$  mV both in the absence and presence of ACh (data not shown).

The voltage dependence of activation was examined in dialyzed neurons by measuring tail current amplitude, using a double pulse protocol. Neurons were held at  $-90$  mV, and brief steps to various test potentials were applied before a hyperpolarizing voltage step to  $-100$  mV. Figure 6A shows  $Ba^{2+}$  currents obtained in the absence and presence of ACh in response to voltage steps to the indicated potentials and the ensuing tail currents elicited on repolarization to  $-100$  mV. The corresponding  $I$ - $V$  relationship obtained for the tail currents of the neuron shown in Fig. 6A are shown in Fig. 6B.  $Ca^{2+}$  channels exhibit sigmoidal activation at potentials positive to  $-40$  mV in both the absence and presence of ACh. Data points were best fit using a two-component Boltzmann distribution

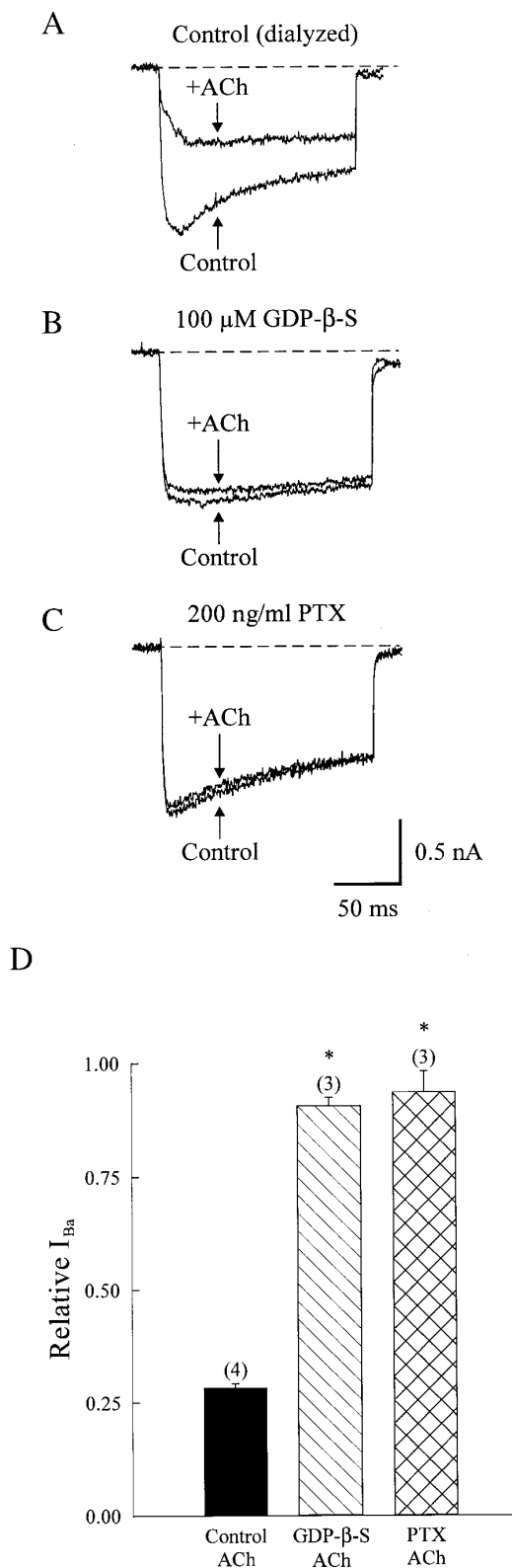


FIG. 5. ACh-mediated inhibition of  $Ca^{2+}$  channels is abolished by pretreatment with pertussis toxin (PTX) or intracellular guanosine 5'-O-(2-thiodiphosphate) trilithium salt (GDP- $\beta$ -S). Superimposed  $Ba^{2+}$  currents elicited by step depolarizations from  $-90$  to  $0$  mV from a neuron dialyzed with either normal pipette solution (A), or a pipette solution containing  $100 \mu\text{M}$  GDP- $\beta$ -S (B), in the absence (Control) and presence of  $100 \mu\text{M}$  ACh (+ACh). The rate of decay of  $I_{Ba}$  was decreased in the presence of GDP- $\beta$ -S, but this was not consistently observed in all neurons. C: superimposed  $I_{Ba}$  evoked by step depolarizations ( $-70$  to  $0$  mV), in the absence (Control) and presence of ACh, from a neuron incubated for 24 h in  $200 \text{ ng/ml}$  PTX. D: bar graph of the mean peak  $I_{Ba}$  amplitude obtained on depolarization from  $-90$  to  $0$  mV in the presence of  $100 \mu\text{M}$  ACh, for neurons dialyzed with a normal pipette solution ( $n = 4$ ), with a pipette solution containing  $100 \mu\text{M}$  GDP- $\beta$ -S ( $n = 3$ ), or preincubated in PTX ( $n = 3$ ). The peak  $I_{Ba}$  amplitude in each condition has been normalized to control (absence of ACh). Asterisk denotes significant difference ( $P < 0.01$ ).

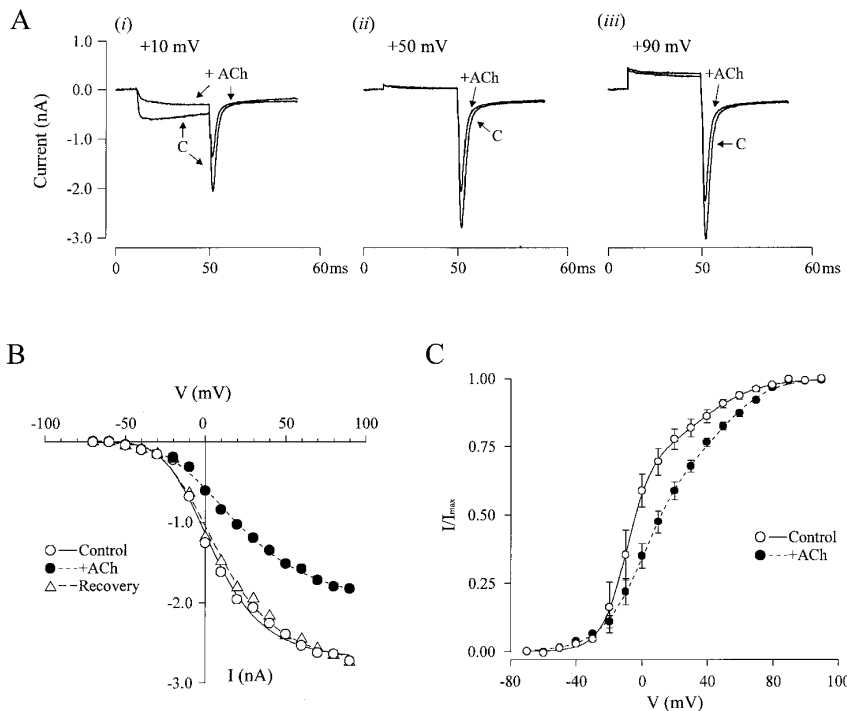


FIG. 6. Effects of muscarinic receptor activation on the voltage dependence of  $\text{Ca}^{2+}$  channel activation. **A**: whole cell  $\text{Ba}^{2+}$  currents evoked by step depolarizations (40 ms duration) to +10 (i), +50 (ii), or +90 mV (iii) from a holding potential of -90 mV in the absence (C) and presence of 100  $\mu\text{M}$  ACh (+ACh). Tail currents recorded after repolarization to -100 mV are displayed on an expanded time scale. **B**:  $I$ - $V$  relation of the  $\text{Ba}^{2+}$  tail currents obtained in the absence (control,  $\circ$ ); recovery,  $\triangle$ ) and presence ( $\bullet$ ) of 100  $\mu\text{M}$  ACh. **C**: relative  $\text{Ba}^{2+}$  tail current amplitude at -100 mV, normalized to maximum  $\text{Ba}^{2+}$  current amplitudes in the absence (control,  $\circ$ ) and presence ( $\bullet$ ) of 100  $\mu\text{M}$  ACh at the various test potentials. Data points are plotted as a function of the voltage of the step depolarization and represent mean  $\pm$  SE for 4 experiments. Curves represent best fit of the data using double Boltzmann distributions with  $i_1$ ,  $i_2$ ,  $V_{h1}$ ,  $V_{h2}$ ,  $k_1$ , and  $k_2$  equal to 0.70, 0.30, -9.7 mV, +35.9 mV, 7.7, and 17.6 for control and 0.71, 0.29, +1.5 mV, +53.2 mV, 13.5, and 14.0 in the presence of ACh, respectively.

$$I_{\text{Ba}} = i_1(I_{\text{Ba}(\text{max})}/\{1 + \exp[(V_{h1} - V)/k_1]\}) + i_2(I_{\text{Ba}(\text{max})}/\{1 + \exp[(V_{h2} - V)/k_2]\})$$

where  $i_1$  and  $i_2$  represent the fraction contributed by each component to the final function. For control,  $i_1$  and  $i_2$  were 0.45 and 0.55, respectively, whereas in the presence of ACh,  $i_1$  and  $i_2$  were 0.19 and 0.82, respectively. Half-maximal activation of the first component ( $V_{h1}$ ) shifted from -7 mV in the absence (Control) to -2 mV in the presence of ACh, whereas the second component ( $V_{h2}$ ) remained relatively constant, +26 mV (Control) and +27 mV (+ACh). The asymptotic maximums predicted from these fits were -2.8 nA for control and -1.9 nA in the presence of ACh, which corresponds to an  $\sim$ 30% reduction of  $I_{\text{Ba}}$  at +90 mV. The effects of ACh on the voltage dependence of  $\text{Ca}^{2+}$  channel activation were completely reversible on wash out.

$\text{Ca}^{2+}$  channel activation curves obtained for four similar experiments are shown in Fig. 6C. Data points represent mean  $I_{\text{Ba}}$  normalized to maximum  $I_{\text{Ba}}$  both in the absence (Control) and presence of ACh (+ACh) and were best fit by a two-component Boltzmann distribution. The relative contributions of the two components of  $I_{\text{Ba}}$  were not markedly changed by ACh; however, in the presence of ACh,  $V_{h1}$  was shifted by +11.2 mV and  $V_{h2}$  by +17.3 mV in the normalized  $\text{Ca}^{2+}$  channel activation curves.

#### Muscarinic ACh modulation of different $\text{Ca}^{2+}$ channel subtypes

The  $\text{Ca}^{2+}$  channel subtype(s) modulated by ACh was examined by determining the amount of ACh-induced inhibition of  $I_{\text{Ba}}$  in the presence of specific  $\text{Ca}^{2+}$  channel antagonists. Rat parasympathetic cardiac neurons have been shown to contain at least three distinct types of  $\text{Ca}^{2+}$  channels, which may be classified pharmacologically: 1) a dihydro-

pyridine-sensitive  $\text{Ca}^{2+}$  channel, 2) an  $\omega$ -CgTX GVIA-sensitive  $\text{Ca}^{2+}$  channel, and 3) a dihydropyridine- and  $\omega$ -CgTX-insensitive  $\text{Ca}^{2+}$  channel (Xu and Adams 1992). Figure 7A shows inward  $\text{Ba}^{2+}$  currents obtained in the absence and presence of ACh, during bath application of PSS, and PSS containing either the dihydropyridine antagonist, nimodipine (10  $\mu\text{M}$ ),  $\omega$ -CgTX-GVIA (300 nM), or  $\text{Cd}^{2+}$  (100  $\mu\text{M}$ ). A plot of  $I_{\text{Ba}}$  amplitude, measured 10 ms after onset of step depolarization to 0 mV, during sequential exposure to different  $\text{Ca}^{2+}$  channel antagonist is shown in Fig. 7B. In the presence of either nimodipine,  $\omega$ -CgTX, or nimodipine +  $\omega$ -CgTX exposure, ACh was able to further inhibit  $I_{\text{Ba}}$ . ACh inhibited  $\sim$ 65% of the inward current remaining during bath application of 10  $\mu\text{M}$  nimodipine, and  $\sim$ 15% of the current that remained in the presence of either  $\omega$ -CgTX or nimodipine +  $\omega$ -CgTX ( $n = 3$ ). Bath application of 100  $\mu\text{M}$   $\text{Cd}^{2+}$  completely inhibited  $I_{\text{Ba}}$ , and the subsequent addition of ACh had no further effect.

#### DISCUSSION

Muscarinic agonists reversibly inhibited high-voltage-activated  $\text{Ca}^{2+}$  channel currents in parasympathetic neurons of neonatal rat intracardiac ganglia. ACh inhibited peak  $I_{\text{Ba}}$  amplitude in a dose-dependent manner with a half-maximal inhibitory concentration of 6 nM and maximal inhibition obtained with 100  $\mu\text{M}$  ACh, in the absence and presence of 70 mM TEA. ACh (100  $\mu\text{M}$ ) reduced peak  $I_{\text{Ba}}$  amplitude by  $\sim$ 75% and altered  $\text{Ca}^{2+}$  channel activation, whereas steady-state inactivation was unaffected.  $\text{Ba}^{2+}$  currents recorded in the absence and presence of muscarinic agonists were completely abolished by external  $\text{Cd}^{2+}$  (100  $\mu\text{M}$ ), indicating that muscarinic agonists are modulating  $\text{Ca}^{2+}$  channel currents. Muscarinic-mediated inhibition of  $\text{Ca}^{2+}$  channel currents has been reported in autonomic neurons, including

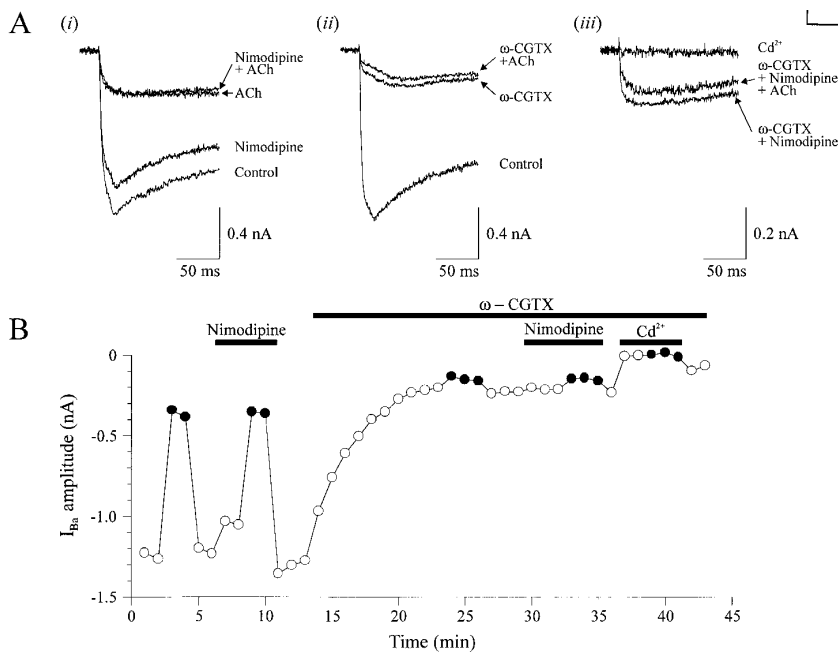


FIG. 7. Differential modulation of  $\text{Ca}^{2+}$  channel subtypes by ACh. *A*: whole cell  $\text{Ba}^{2+}$  currents evoked by step depolarizations to +5 mV from a holding potential of -70 mV in the absence and presence of the indicated  $\text{Ca}^{2+}$  channel antagonists. Nimodipine (10  $\mu\text{M}$ ; *i*),  $\omega$ -conotoxin-GVIA ( $\omega$ -CgTX; 300 nM; *ii*),  $\omega$ -CgTX + nimodipine, and  $\text{Cd}^{2+}$  (100  $\mu\text{M}$ ) (*iii*) were bath applied, and ACh (100  $\mu\text{M}$ ) was pressure ejected from an extracellular pipette. *B*:  $\text{Ba}^{2+}$  current amplitude plotted as a function of time during sequential bath perfusion with normal physiological salt solution (PSS) or PSS containing the indicated  $\text{Ca}^{2+}$  channel antagonists in the absence ( $\circ$ ) and presence ( $\bullet$ ) of 100  $\mu\text{M}$  ACh.  $I_{\text{Ba}}$  current amplitude was measured 10 ms from the onset of the step depolarization.

rat sympathetic (Bernheim et al. 1992; Wanke et al. 1987) and bullfrog parasympathetic (Tse et al. 1990) neurons. In sympathetic neurons from rat superior cervical ganglia (SCG), muscarinic inhibition of  $I_{\text{Ca}}$  was shown to be sensitive to pirenzepine (<120 nM), suggesting that the  $I_{\text{Ba}}$  inhibition was mediated by activation of the  $M_1$  muscarinic receptor subtype (Wanke et al. 1987). However, a recent study in rat SCG sympathetic neurons showed that the activation of both  $M_1$  and  $M_4$  receptor subtypes mediate the inhibition of  $\text{Ca}^{2+}$  channel currents (Bernheim et al. 1992). In NG108-15 neuroblastoma  $\times$  glioma hybrid cells transfected with cDNA encoding for m1-m4 muscarinic AChR subtypes,  $M_2$  and  $M_4$  receptor activation inhibited  $\text{Ba}^{2+}$  currents, whereas  $M_1$  and  $M_3$  receptor activation had no effect (Higashida et al. 1990). The discrepancy regarding the receptor subtype involved may have arisen, in part, from the similar pharmacological profiles of the muscarinic receptors, particularly  $M_1$  and  $M_4$ . For example, the pirenzepine concentrations used by Wanke et al. (1987) to inhibit  $M_1$  receptors may also antagonize  $M_4$  receptors in rat sympathetic neurons, particularly because similar pirenzepine concentrations block  $M_4$  receptor-mediated depression of  $I_{\text{Ca}}$  in transfected NG108-15 cells (Caulfield and Brown 1991).

In the present study, the use of selective muscarinic receptor antagonists suggest that  $M_4$  receptor activation inhibits  $\text{Ca}^{2+}$  channel currents in rat intracardiac neurons. The  $M_2$  muscarinic receptor antagonist, AF-DX 116 (300 nM), failed to inhibit ACh-induced attenuation of  $\text{Ca}^{2+}$  channel currents. Given that the  $K_d$  for inhibition of  $M_2$  muscarinic receptors by AD-FX 116 was shown to be 200 nM in Chinese Hamster Ovary (CHO) cells transfected with the m2 muscarinic receptor gene (Hulme et al. 1990), it is unlikely that the attenuation of  $\text{Ca}^{2+}$  channel currents in rat intracardiac neurons is mediated by  $M_2$  muscarinic receptors. ACh-evoked inhibition of  $I_{\text{Ba}}$  was, however, antagonized by pirenzepine (300 nM), in contrast to observations in bullfrog intracardiac neurons where pirenzepine  $\leq 100 \mu\text{M}$  had no

effect (Tse et al. 1990). Pirenzepine at a concentration of 300 nM has been shown to inhibit the activation of both  $M_1$  ( $K_d = 16$  nM) and  $M_4$  ( $K_d = 80$  nM) muscarinic receptor subtypes (Caulfield and Brown 1991; Hulme et al. 1990). However, the selective  $M_1$  muscarinic receptor antagonist, m1-toxin, failed to inhibit ACh-mediated attenuation of  $I_{\text{Ba}}$  at a concentration sufficient to antagonize  $M_1$  muscarinic receptor-mediated inhibition of  $I_{\text{M}}$  in these neurons (Cuevas et al. 1997). Further evidence suggesting that ACh-induced inhibition of  $I_{\text{Ba}}$  is mediated by  $M_4$  receptor activation is the observation that m4-toxin, specific for the m4/ $M_4$  muscarinic receptor subtype (Jolkkonen et al. 1994; Max et al. 1993b), antagonizes muscarine-induced depression of  $\text{Ca}^{2+}$  channel currents in a dose-dependent manner with a half-maximally effective concentration of 11 nM. Together these data suggest that ACh-induced attenuation of  $\text{Ca}^{2+}$  channel currents in cardiac neurons is mediated exclusively by  $M_4$  muscarinic receptors.

Muscarinic agonist attenuation of  $\text{Ca}^{2+}$  channel currents via the  $M_4$  receptor activation is mediated by a PTX-sensitive G-protein. ACh-induced depression of  $I_{\text{Ba}}$  was abolished by either intracellular dialysis with GDP- $\beta$ -S or preincubation of the neurons with PTX. In contrast, ACh modulation of  $I_{\text{M}}$  and discharge activity that is mediated by  $M_1$  muscarinic receptor activation in rat intracardiac neurons was not inhibited by PTX (J. Cuevas and D. J. Adams, unpublished observations). A PTX-sensitive effector coupling of muscarinic receptor activation to the inhibition of  $\text{Ca}^{2+}$  channel currents has been previously described in rat sympathetic neurons (Bernheim et al. 1992; Wanke et al. 1987) and bullfrog parasympathetic neurons (Tse et al. 1990). Furthermore, only the  $M_4$  receptor subtype has been shown to inhibit  $I_{\text{Ca}}$  via a PTX-sensitive pathway (Bernheim et al. 1992; Higashida et al. 1990). In rat intracardiac neurons, PTX-sensitive G-proteins have been shown to mediate norepinephrine inhibition of  $\text{Ca}^{2+}$  channel currents (Xu and Adams 1993). The attenuation of  $I_{\text{Ba}}$  by norepinephrine and ACh was not addi-

tive (data not shown), suggesting a convergence in the signal transduction pathways, similar to that reported in NG 108-15 cells transfected with the  $M_4$  receptor, where ACh and norepinephrine have mutually occlusive interactions (Higashida et al. 1990).

Intracellular dialysis of the voltage-clamped neurons with a pipette solution containing the  $\text{Ca}^{2+}$  chelator BAPTA, failed to inhibit muscarinic agonist-induced inhibition of  $I_{\text{Ba}}$ , suggesting that cytosolic  $\text{Ca}^{2+}$  is not involved in the signal transduction pathway coupling muscarinic receptors to suppression of  $\text{Ca}^{2+}$  channels. In contrast, a BAPTA-sensitive pathway has been implicated in the slow muscarinic inhibition of  $\text{Ca}^{2+}$  channels observed in rat sympathetic neurons (Bernheim et al. 1992). However, the inhibition mediated by this pathway has been attributed to  $M_1$  and not  $M_4$  muscarinic receptor activation and is PTX insensitive (Bernheim et al. 1992). Previous studies have demonstrated that neither diacylglycerol, protein kinase C, nor adenylate cyclase activation have any significant effects on  $\text{Ca}^{2+}$  channel currents in rat intracardiac neurons (Xu and Adams 1993). Activation of a PTX-sensitive G-protein(s) has been proposed to inhibit  $I_{\text{Ca}}$  via direct interaction with  $\text{Ca}^{2+}$  channels (see Hille 1994). This putative mechanism had been proposed for the muscarinic receptor inhibition of  $\text{Ca}^{2+}$  channel currents in bullfrog intracardiac neurons (Tse et al. 1990) and is consistent with the results of the present study.

Under control conditions,  $\text{Ca}^{2+}$  channel currents reached their peak within  $\sim 10$  ms and exhibited a biphasic time course of decay (see Xu and Adams 1992). In the presence of ACh, the activation of  $\text{Ca}^{2+}$  channel currents was slowed, and the rapidly inactivating component of  $I_{\text{Ba}}$  decay was abolished. The decay of  $I_{\text{Ba}}$  was best fit by a single exponential function ( $\tau_s$ ) similar to that described by norepinephrine modulation of  $\text{Ca}^{2+}$  currents in rat intracardiac neurons (Xu and Adams 1993). Steady-state inactivation of voltage-dependent  $\text{Ca}^{2+}$  channels in rat intracardiac neurons was unaffected by ACh. The voltage dependence of  $\text{Ca}^{2+}$  channel activation was shifted to more positive potentials by ACh. In the absence and presence of ACh, the voltage dependence of activation was best fit by the sum of two Boltzmann distributions, and ACh shifted the half-maximal potential for the components by +11.2 and +17.3 mV, respectively. In bullfrog intracardiac neurons, the voltage dependence of  $\text{Ca}^{2+}$  channels was similarly shifted to more positive potentials in the presence of ACh (Tse et al. 1990). However, a shift of  $\text{Ca}^{2+}$  channel gating to more positive potentials, which require stronger depolarizations to open, is not sufficient to account for the ACh-induced inhibition of  $I_{\text{Ba}}$  observed in rat intracardiac neurons (see Fig. 6) (Bean 1989). Peak  $\text{Ca}^{2+}$  channel tail current amplitude obtained in the presence of ACh was reduced by  $\geq 30\%$ , relative to control at +90 mV, indicating a voltage-independent component of the attenuation of  $\text{Ca}^{2+}$  channel activation. Similarly, ACh has been shown to inhibit  $\text{Ca}^{2+}$  channels through both voltage-dependent and -independent mechanisms in rat sympathetic neurons (Mathie et al. 1992).

Application of ACh inhibited primarily the  $\omega$ -CgTX GVIA-sensitive  $\text{Ca}^{2+}$  channels that are responsible for the rapidly inactivating component of  $I_{\text{Ba}}$ .  $\omega$ -CgTX GVIA-sensitive (N-type)  $\text{Ca}^{2+}$  channels constitute  $\sim 75\%$  of the total  $\text{Ca}^{2+}$  channel current (Xu and Adams 1992), but ACh also

depressed dihydropyridine-sensitive (L-type) and  $\omega$ -CgTX GVIA- and dihydropyridine-insensitive  $\text{Ca}^{2+}$  channel currents. Norepinephrine also inhibited N-type  $\text{Ca}^{2+}$  channels in rat intracardiac neurons via a PTX-sensitive G-protein mechanism (Xu and Adams 1993). In rat sympathetic neurons, however, the  $M_4$  receptor-mediated, PTX-sensitive pathway inhibits N-type  $\text{Ca}^{2+}$  channels exclusively (Bernheim et al. 1992; Mathie et al. 1992; Wanke et al. 1987).

#### Functional significance

Cholinergic (vagal) innervation of mammalian intracardiac ganglia primarily involves axosomatic synapses (Ellison and Hibbs 1976), and therefore the investigation of ACh modulation of voltage-dependent  $\text{Ca}^{2+}$  channels in the cell soma is relevant to autonomic transmission. ACh-mediated inhibition of  $\text{Ca}^{2+}$  channel currents may regulate transmitter release from both intrinsic and extrinsic presynaptic nerve terminals within intracardiac ganglia and to cardiac muscle.  $M_4$  muscarinic receptor inhibition of a heterogeneous population of  $\text{Ca}^{2+}$  channels may be physiologically significant, given that neurally evoked transmitter release in rat parasympathetic ganglia is not inhibited by  $\omega$ -CgTX GVIA but is suppressed by  $\text{Cd}^{2+}$  block of  $\text{Ca}^{2+}$  channels (Seabrook and Adams 1989). The stimulation of muscarinic receptors on sympathetic nerve terminals in the heart reduce the release of norepinephrine (Foldes et al. 1989; Löffelholz and Muscholl 1969; Manabe et al. 1991; Vizi et al. 1989), whereas atropine enhances vagal-stimulated ACh release in the intact mammalian myocardium (Löffelholz and Muscholl 1969; Wetzel et al. 1985). In sympathetic neurons,  $\alpha$ -adrenergic inhibition of  $I_{\text{Ca}}$  may underlie depression of norepinephrine release and provide negative feedback regulation (Lipscombe et al. 1989). Given that acetylcholine is the principal neurotransmitter mediating vagal innervation of the heart, the presence of this muscarinic ACh-mediated  $\text{Ca}^{2+}$  channel inhibitory mechanism suggests that it may also provide negative feedback regulation.

We thank Dr. Lincoln Potter for purifying and supplying the  $m1$ - and  $m4$ -toxins.

This research was supported by National Heart, Lung, and Blood Institute Grant HL-35422 and National Health and Medical Research Council of Australia Grant 961138.

Present address of J. Cuevas: Dept. of Biology, University of California, San Diego, La Jolla, CA 92093.

Address for reprint requests: D. J. Adams, Dept. of Physiology and Pharmacology, University of Queensland, Brisbane, QLD 4072, Australia.

E-mail: dadams@plpk.uq.edu.au

Received 29 January 1997; accepted in final form 20 June 1997.

#### REFERENCES

- ALLEN, T.G.J. AND BURNSTOCK, G.  $M_1$  and  $M_2$  muscarinic receptors mediate excitation and inhibition of guinea-pig intracardiac neurons in culture. *J. Physiol. (Lond.)* 422: 463–480, 1990.
- ALLEN, T.G.J., HASSALL, C.J.S., AND BURNSTOCK, G. Mammalian intrinsic cardiac neurons in cell culture. In: *Neurocardiology*, edited by J. A. Armour and J. L. Ardell. New York: Oxford Univ. Press, 1994, p. 115–138.
- BEAN, B. P. Neurotransmitter inhibition of neuronal calcium currents by changes in channel voltage dependence. *Nature* 340: 153–156, 1989.
- BEECH, D. J., BERNHEIM, L., MATHIE, A., AND HILLE, B. Intracellular  $\text{Ca}^{2+}$  buffers disrupt muscarinic suppression of  $\text{Ca}^{2+}$  current and M current in rat sympathetic neurons. *Proc. Natl. Acad. Sci. USA* 88: 652–656, 1991.

- BERNHEIM, L., BEECH, D., AND HILLE, B. A diffusible second messenger mediates one of the pathways coupling receptors to calcium channels in rat sympathetic neurons. *Neuron* 6: 859–867, 1991.
- BERNHEIM, L., MATHIE, A., AND HILLE, B. Characterization of muscarinic receptor subtypes inhibiting  $Ca^{2+}$  current and M current in rat sympathetic neurons. *Proc. Natl. Acad. Sci. USA* 89: 9544–9548, 1992.
- CAULFIELD, M. P. Muscarinic receptor-mediated inhibition of voltage-activated  $Ca$ -current in neuroblastoma  $\times$  glioma hybrid (NG 108-15) cells—reduction of muscarinic agonist and antagonist activity by tetraethylammonium (TEA). *Neurosci. Lett.* 127: 165–168, 1991.
- CAULFIELD, M. P. AND BROWN, D. A. Pharmacology of the putative  $M_4$  muscarinic receptor mediating  $Ca$ -current inhibition in neuroblastoma  $\times$  glioma hybrid (NG 108-15) cells. *Br. J. Pharmacol.* 104: 39–44, 1991.
- CUEVAS, J. AND ADAMS, D. J.  $M_4$  muscarinic receptor activation modulates voltage-dependent calcium conductances in isolated rat intracardiac neurones (Abstract). *J. Physiol. (Lond.)* 487: 122P, 1995.
- CUEVAS, J., HARPER, A. A., TREQUATRINI, C., AND ADAMS, D. J. Passive and active membrane properties of isolated rat intracardiac neurons: regulation by H- and M-currents. *J. Neurophysiol.* 78: 1890–1902, 1997.
- ELLISON, J. P. AND HIBBS, R. G. An ultrastructural study of mammalian cardiac ganglia. *J. Mol. Cell. Cardiol.* 8: 89–101, 1976.
- FIEBER, L. A. AND ADAMS, D. J. Acetylcholine-evoked currents in cultured neurones dissociated from rat parasympathetic cardiac ganglia. *J. Physiol. (Lond.)* 434: 215–237, 1991.
- FOLDES, F. F., KOBAYASHI, O., KINJO, M., HARSING, L. G., JR., NAGASHIMA, H., DUNCALF, D., GOLDINER, P. L., AND VIZI, E. S. Presynaptic effect of muscle relaxants on the release of  $^3H$ -noradrenaline controlled by endogenous acetylcholine in guinea pig atrium. *J. Neural Transm.* 76: 169–180, 1989.
- GÄHWILER, B. H. AND BROWN, D. A. Muscarine affects calcium-currents in rat hippocampal pyramidal cells in vitro. *Neurosci. Lett.* 76: 301–306, 1987.
- HAMILL, O. P., MARTY, A., NEHER, E., SAKMANN B., AND SIGWORTH, F. J. Improved patch-clamp techniques for high-resolution current recording from cells and cell-free membrane patches. *Pflügers Arch.* 391: 85–100, 1981.
- HASSALL, C.J.S., STANFORD, S. C., BURNSTOCK, G., AND BUCKLEY, N. J. Co-expression of four muscarinic receptor genes by the intrinsic neurons of the rat and guinea-pig heart. *Neuroscience* 56: 1041–1048, 1993.
- HIGASHIDA, H., HASHII, M., FUKUDA, K., CAULFIELD, M. P., NUMA, S., AND BROWN, D. A. Selective coupling of different muscarinic acetylcholine receptors to neuronal calcium currents in DNA-transfected cells. *Proc. R. Soc. Lond. B Sci.* 242: 68–74, 1990.
- HILLE, B. Modulation of ion-channel function by G-protein-coupled receptors. *Trends Neurosci.* 17: 531–536, 1994.
- HOOVER, D. B., BAISDEN, R. H., AND XI-MOY, S. X. Localization of muscarinic receptor mRNAs in rat heart and intrinsic cardiac ganglia by in situ hybridization. *Circ. Res.* 75: 813–820, 1994.
- HULME, E. C., BIRDSALL, N.J.M., AND BUCKLEY, N. J. Muscarinic receptor subtypes. *Annu. Rev. Pharmacol. Toxicol.* 30: 633–673, 1990.
- JOLKKONEN, M., VAN GIERSBERGEN, P. L., HELLMAN, U., WERNSTEDT, C., AND KARLSSON, E. A toxin from the green mamba *Dendroaspis angusticeps*: amino acid sequence and selectivity for muscarinic  $m_4$  receptors. *FEBS Lett.* 532: 91–94, 1994.
- LIPSCOMBE, D., KONGSAMUT, S., AND TSIEN, R. W.  $\alpha$ -Adrenergic inhibition of sympathetic neurotransmitter release mediated by modulation of N-type calcium-channel gating. *Nature* 340: 639–642, 1989.
- LÖFFELHOLZ, K. AND MUSCHOLL, E. A muscarinic inhibition of the noradrenaline release evoked by postganglionic sympathetic nerve stimulation. *Naunyn-Schmiedeberg's Arch. Pharmacol.* 265: 1–15, 1969.
- LÖFFELHOLZ, K. AND PAPPANO, A. J. The parasympathetic neuroeffector junction of the heart. *Pharmacol. Rev.* 37: 1–18, 1985.
- MCDONOUGH, P. M., WETZEL, G. T., AND BROWN, J. H. Further characterization of the presynaptic alpha-1-receptor modulating  $^3H$ -ACh release from rat atria. *J. Pharmacol. Exp. Ther.* 238: 612–617, 1986.
- MANABE, N., FOLDES, F. F., TOROCSIK, A., NAGASHIMA, H., GOLDINER, P. L., AND VIZI, E. S. Presynaptic interaction between vagal and sympathetic innervation in the heart: modulation of acetylcholine and noradrenaline release. *J. Auton. Nerv. Syst.* 32: 233–242, 1991.
- MATHIE, A., BERNHEIM, L., AND HILLE, B. Inhibition of N- and L-type calcium channels by muscarinic receptor activation in rat sympathetic neurons. *Neuron* 8: 907–914, 1992.
- MAX, S. I., LIANG, J. S., AND POTTER, L. T. Purification and properties of m1-toxin, a specific antagonist of m1 muscarinic receptors. *J. Neurosci.* 13: 4293–4300, 1993a.
- MAX, S. I., LIANG, J.-S., PURKERSON, S. L., AND POTTER, L. T. m4-toxin, a selective, reversible, allosteric antagonist of m4 muscarinic receptors. *Soc. Neurosci. Abstr.* 19: 462, 1993b.
- MIHARA, S., IKEDA, K., AND NISHI, S. Muscarinic  $M_2$  receptors on cardiac ganglion neurons of the guinea-pig heart. *Kurume Med. J.* 35: 183–192, 1988.
- RAE, J., COOPER, K., GATES, P., AND WATSKY, M. Low access resistance perforated patch recordings using amphotericin B. *J. Neurosci. Methods* 37: 15–26, 1991.
- SEABROOK, G. R. AND ADAMS, D. J. Inhibition of neurally-evoked transmitter release by calcium channel antagonists in rat parasympathetic ganglia. *Br. J. Pharmacol.* 97: 1125–1136, 1989.
- TSE, A., CLARK, R. B., AND GILES, W. R. Muscarinic modulation of calcium current in neurones from the interatrial septum of bull-frog heart. *J. Physiol. (Lond.)* 427: 127–149, 1990.
- VIZI, E. S., KOBAYASHI, O., TOROCSIK, A., KINJO, M., NAGASHIMA, H., MANABE, N., GOLDINER, P. L., POTTER, P. E., AND FOLDES, F. F. Heterogeneity of presynaptic muscarinic receptors involved in modulation of transmitter release. *Neuroscience* 31: 259–267, 1989.
- WANKE, E., FERRONI, A., MALGAROLI, A., AMROSINI, A., POZZAN, T., AND MELDOLESI, J. Activation of a muscarinic receptor selectively inhibits a rapidly inactivated  $Ca^{2+}$  current in rat sympathetic neurons. *Proc. Natl. Acad. Sci. USA* 84: 4313–4317, 1987.
- WETZEL, G. T., GOLDSTEIN, D., AND BROWN, J. H. Cardiac acetylcholine release can be regulated through alpha-1-adrenergic receptor. *Circ. Res.* 56: 763–766, 1985.
- XU, Z.-J. AND ADAMS, D. J. Voltage-dependent sodium and calcium currents in cultured parasympathetic neurones from rat intracardiac ganglia. *J. Physiol. (Lond.)* 456: 425–441, 1992.
- XU, Z.-J. AND ADAMS, D. J.  $\alpha$ -Adrenergic modulation of ionic currents in cultured parasympathetic neurons from rat intracardiac ganglia. *J. Neurophysiol.* 69: 1060–1070, 1993.